Learning collaborative manipulation tasks by demonstration using a haptic interface

Sylvain Calinon, Paul Evrard, Elena Gribovskaya, Aude Billard,
Abderrahmane Kheddar

▶ **To cite this version:**

Learning collaborative manipulation tasks by demonstration using a haptic interface

Sylvain Calinon, Paul Evrard, Elena Gribovskaya, Aude Billard, Abderrahmane Kheddar

Abstract— **This paper presents a method by which a robot can learn through observation to perform a collaborative manipulation task, namely lifting an object. The task is first demonstrated by a user controlling the robot's hand via a haptic interface. Learning extracts statistical redundancies in the examples provided during training by using Gaussian Mixture Regression and Hidden Markov Model. Haptic communication reflects more than pure dynamic information on the task, and includes communication patterns, which result from the two users constantly adapting their hand motion to coordinate in time and space their respective motions. We show that the proposed statistical model can efficiently encapsulate typical communication patterns across different dyads of users, that are stereotypical of collaborative behaviours between humans and robots. The proposed learning approach is generative and can be used to drive the robot's retrieval of the task by ensuring a faithful reproduction of the overall dynamics of the task, namely by reproducing the force patterns for both lift the object and adapt to the human user's hand motion. This work shows the potential that teleoperation holds for transmitting both dynamic and communicative information on the task, which classical methods for programming by demonstration have traditionally overlooked.**
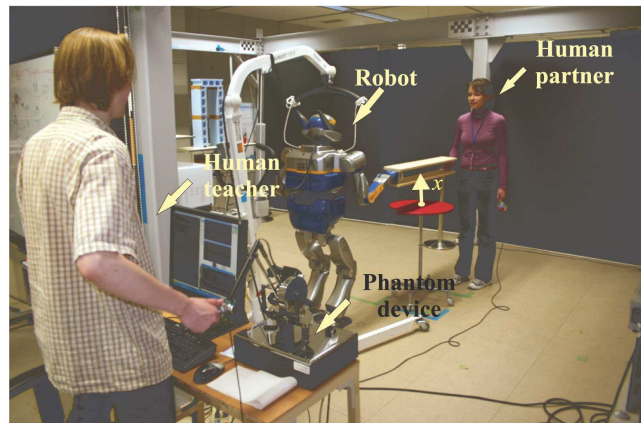
Fig. 1. Experimental setup. A user (on the left) teleoperates a humanoid robot to demonstrate how to perform a lifting task collaboratively with another user (on the right).

I. INTRODUCTION

Recent research in robotics reveals a constantly increasing interest to the problem of physical robot-human interaction, where a robot and a human are contacting with each other either directly or through an object. Endowing robots with the ability to collaborate with human partners in a smooth and natural way will greatly promote the use of robots in user-centered applications, which assume dynamic environments and the haptic contact between agents.

Various conventional methods were proposed in last decades to address robot-human interaction [1]–[4]. A common approach consists of implementing impedance or admittance controllers following desired dynamics imposed by a user [1]. Such schemes have been extended with varying impedance parameters, or with identification of the jerk parameters best fitting a trajectory followed by a human operator, with subsequent tracking of a reference trajectory generated with the identified parameters [5], [6].

Although the above-mentioned approach has been successfully implemented in certain applications, it is rather restrictive as the robot is always assigned a follower role with respect to a human partner. For transmitting both dynamic and communicative information on the task, we propose here to learn a controller for the robot by imitation [7], where a user provides demonstrations of the collaborative skill through a haptic device (see Fig. 7).

We adopt a conventional terminology [8]–[10] and consider as a "leader" a partner planning the motion and as a "follower" a partner whose behavior is reactive with respect to the task plan imposed by the leader. A robot being constantly a follower puts more pressure on a human partner, as besides concentrating on the task goals he/she has to be constantly aware about the robot's physical capabilities and constraints (e.g. to avoid bringing it to an unfavorable posture). Furthermore advanced robotic platforms are equipped with various sensors allowing to gather more detailed and complete information about an environment. Therefore, in certain conditions, the robot should be able to switch to a leading behavior and guide the human partner (e.g., if an obstacle reduces the field of view of the operator or a task requires precise positioning). Developing such controllers requires the understanding and interpretation of the underlying processes of haptic communication. Reed *et al* reported experiments showing that dyads of human users exhibit specialization during collaboration that can be seen as a role switching between the partners during the task [11]. In a previous work of ours, a generic model has been proposed

that encompasses this phenomenon and may encapsulate different patterns of role switching [12]. However, this model requires knowledge about strategies in the role attribution during collaborative tasks in order to implement advanced collaborative behaviors on robotic platforms.

We present here preliminary results towards building a statistical framework based on *Hidden Markov Model* (HMM) and *Gaussian Mixture Regression* (GMR) [13], [14] allowing to extract both leading and following behaviors from task demonstrations. We take the perspective that by encoding probabilistically the correlations between the dynamical signals (forces) and kinematic parameters of the task in a continuous manner, the robot can autonomously select a controller to reproduce the collaborative skill with an appropriate behavior.

Wang *et al* recently suggested the use of discrete HMMs to automatically detect whether the human partner was acting actively or passively during handshaking between a robotic system and a human operator [15]. The behavior of the robot was then modified accordingly. In our work, continuous HMMs are used to represent both task motion and user's haptic communication signals in the same framework.

II. EXPERIMENTAL SETUP

A. Teaching scenario

We propose to teach a robot how to perform a collaborative lifting task. The task consists of lifting a rigid beam in a collaborative way and by keeping the beam horizontal. In the first set of recordings, the teacher is asked to close his eyes while moving the robot's hand and the other user has the role of initiating and terminating the motion (i.e. robot is following). The second set of recordings is the symmetric case where the teacher has the role of initiating and terminating the motion while the other user is blindfolded (i.e. robot is leading).

B. Hardware setup

The collaborative lifting task is demonstrated to a HRP-2 humanoid robot. HRP-2 is a full size humanoid with 30 degrees of freedom (dof): 6 dof for each leg, 6 dof for each arm, 2 dof for the chest, 2 dof for the head and 1 dof for each gripper. Only the right arm is used to perform the task, while the robot is standing. We assume that the hand holds the object firmly enough so that the object can only translate vertically with the hand of the robot. The motion of the wrist is constrained to move only along a vertical direction during the whole task, while its orientation is constrained to remain constant.

In order to perform the demonstrations, the teacher teleoperates the robot using a PHANToM Premium device with 6 dof force/torque feedback. Hence, the teacher has a full feedback of the interaction wrench measured at the gripper of the robot. PHANToM devices are impedance type devices, meaning that they are low friction, low inertia mechanisms, and accept force and torque references. The haptic device used for the demonstration is a Premium 1.5 model with workspace of $381mm$ x $267mm$ x $191mm$. A slight rescaling was necessary to map the workspace of the PHANToM device to the workspace of the robot.

C. Controller

As PHANToM devices accept force/torque references, a natural coupling scheme is a bilateral 2-channel Velocity-Force coupling. Hence, the velocity of the tip of the PHANToM device are measured and sent as a velocity reference to the robot. Forces are measured at the wrists of the robot, and the corresponding wrench at the gripper is sent as a reference to the PHANToM device. The control law for the haptic device is thus

$$F_m = U \ K_f \ F_s, \qquad (1)$$

where F_m is the reference force sent to the PHANToM device, F_s is the wrench at the gripper of the robot, K_f is a diagonal gain matrix, and U is a transformation matrix from the coordinates frame in which the sensor force is measured to the PHANToM coordinates frame.

The robot is teleoperated using the following law

$$\dot{q} = J^\dagger \ U^{-1} \ v_h, \qquad (2)$$

where $J^\dagger$ is the Jacobian pseudoinverse of the robot's gripper position with respect to the angular velocities of the right arm, v_h is the velocity of the handle of the PHANToM device, and $\dot{q}$ is a joint velocity reference that is integrated and sent to the lower level proportional-derivative joint position controller of the robot.

III. PROBABILISTIC MODEL

A. Learning

Data gathered during demonstrations entail position x and velocities $\dot{x}$ of the robot's hand, as well as the force F_S sensed at the level of its wrist. If F_s is the force recorded by the force sensor and by considering that the object is horizontal and held symmetrically by the two partners,[1] i.e. that the weight of the object is shared equally between the two partners. The force component due to the mass of the object is eliminated by computing the interaction force F as

$$F = F_s - \frac{m}{2}(\ddot{x} - g), \qquad (3)$$

where g is the standard gravity constant.[2] Only motions in the vertical plane are considered in the experiment ($x, \dot{x}, F \in \mathbb{R}$), but the framework can be used with multiple degrees of freedom (see illustrative examples in Fig. 3 and 4). The frame of reference is pointing upward (i.e. if the user lifts the object while the hand does not move, F becomes positive). The dataset is thus composed of a set of datapoints $\xi = [x, \dot{x}, F]$.

The joint distribution $\mathcal{P}(x, \dot{x}, F)$ is encoded in a *Hidden Markov Model* (HMM) of K states, where the output

---

[1]This remains reasonable as the contact with the object is achieved through two similar handles placed on both sides of the object.

[2]The mass of the object was here known in advance, but it can also be estimated at the beginning of the interaction when the object is already handled by the two partners but does not move yet (null acceleration).
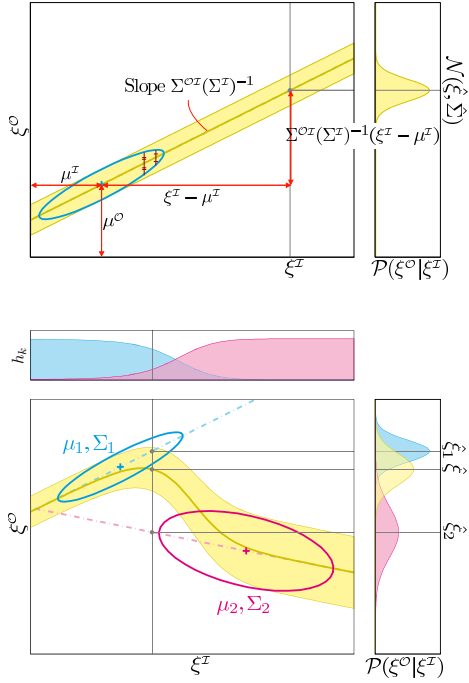
Fig. 2. Schematic of the Gaussian Mixture Regression (GMR) process. *Top:* By considering a single Gaussian distribution. *Bottom:* By considering a GMM composed of two Gaussian distributions.
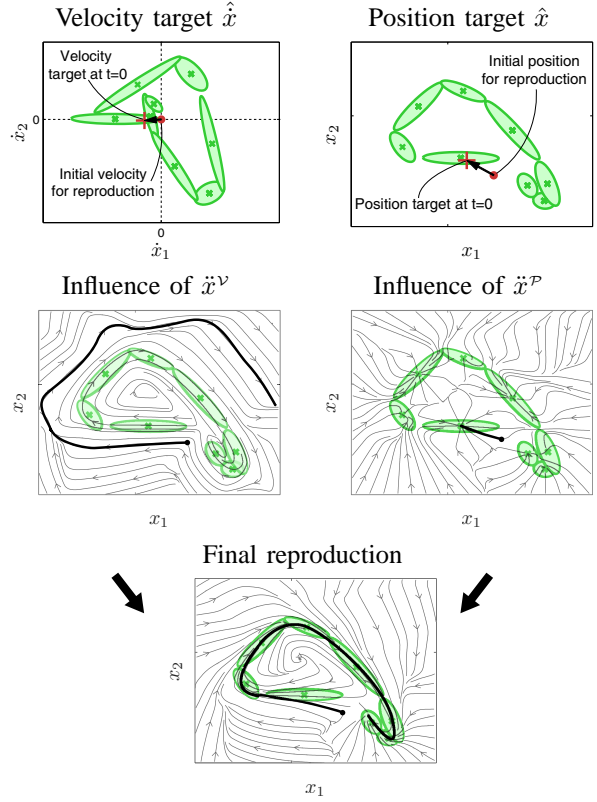

Fig. 3. Example of a dynamical system used to reproduce a demonstrated motion by starting from a different initial position. A 2D motion is considered here as an illustrative example. The first row shows the HMM in velocity and position space encoding the $\{\dot{x}, x\}$ relationships. In the second and third row, the initial positions are represented by points and the retrieved trajectories are represented in bold line.

distribution of each state is represented by a Gaussian distribution representing locally the correlations between the different variables. The parameters of the model $\{\Pi, a, \mu, \Sigma\}$ are learned through *Baum-Welch* algorithm, a variant of Expectation-Maximization (EM) for HMM [16]. Π_i is the initial probability of being in state i, a_{ij} is the probability to transit from state i to state j. μ_i and Σ_i represent the center and covariance matrix of the i-th Gaussian distribution of the HMM with K states. The different variables of the dataset and associated model are labelled separately as

$$\begin{bmatrix} \xi^{\mathcal{I}} \\ \xi^{\mathcal{O}} \end{bmatrix} = \begin{bmatrix} x \\ F \\ \dot{x} \end{bmatrix}, \begin{bmatrix} \xi^{\mathcal{O}'} \\ \xi^{\mathcal{I}'} \end{bmatrix} = \begin{bmatrix} x \\ F \\ \dot{x} \end{bmatrix},$$

$$\begin{bmatrix} \mu_i^{\mathcal{I}} \\ \mu_i^{\mathcal{O}} \end{bmatrix} = \begin{bmatrix} \mu_i^x \\ \mu_i^F \\ \mu_i^{\dot{x}} \end{bmatrix}, \begin{bmatrix} \Sigma_i^{\mathcal{I}} & \Sigma_i^{\mathcal{IO}} \\ \Sigma_i^{\mathcal{OI}} & \Sigma_i^{\mathcal{O}} \end{bmatrix} = \begin{bmatrix} \Sigma_i^x & \Sigma_i^{xF} & \Sigma_i^{x\dot{x}} \\ \Sigma_i^{Fx} & \Sigma_i^F & \Sigma_i^{F\dot{x}} \\ \Sigma_i^{\dot{x}x} & \Sigma_i^{\dot{x}F} & \Sigma_i^{\dot{x}} \end{bmatrix},$$

$$\begin{bmatrix} \mu_i^{\mathcal{O}'} \\ \mu_i^{\mathcal{I}'} \end{bmatrix} = \begin{bmatrix} \mu_i^x \\ \mu_i^F \\ \mu_i^{\dot{x}} \end{bmatrix}, \begin{bmatrix} \Sigma_i^{\mathcal{O}'} & \Sigma_i^{\mathcal{OI}'} \\ \Sigma_i^{\mathcal{IO}'} & \Sigma_i^{\mathcal{I}'} \end{bmatrix} = \begin{bmatrix} \Sigma_i^x & \Sigma_i^{xF} & \Sigma_i^{x\dot{x}} \\ \Sigma_i^{Fx} & \Sigma_i^F & \Sigma_i^{F\dot{x}} \\ \Sigma_i^{\dot{x}x} & \Sigma_i^{\dot{x}F} & \Sigma_i^{\dot{x}} \end{bmatrix},$$

where the uppercase indices x, F and $\dot{x}$ refer respectively to position, force and velocity components.[3]

Fig. 4. Influence of the variability observed during demonstrations for the reproduction of the skill. To illustrate the influence of consistency across the different observations, two datasets have first been generated from one reference 2-dimensional trajectory (in dashed line), where an HMM of 5 states is trained on each dataset. The first dataset consists of 10 trajectories with strong consistency among the different demonstrations (*first graph*). The second dataset presents more variability (*second graph*). For each of the two models, two reproductions are then computed by starting from new initial positions (*third graph*). The two trajectories in black line are retrieved with the HMM represented in first graph, while the two trajectories in grey line are retrieved by the HMM represented in second graph.

---

[3]Note that this process can similarly be used to encode trajectories defined by position and velocity recordings (i.e. without force), where we simply have $\xi^{\mathcal{I}} = x$ and $\xi^{\mathcal{O}} = \dot{x}$.

B. Reproduction

During reproduction, at each time step the current observation $\xi = [x, \dot{x}, F]$ is used to define a weight factor h_i representing the influence of the i-th state

$$h_i(\xi_t) = \frac{\alpha_{i,t}}{\sum_{k=1}^K \alpha_{k,t}}, \tag{4}$$

$$\text{with} \quad \alpha_{i,t} = \left(\sum_{k=1}^K \alpha_{k,t-1} \, a_{ki} \right) \mathcal{N}(\xi_t; \, \mu_i, \Sigma_i),$$

where $\alpha_{i,t}$ is the *forward* variable (defined recursively through the HMM representation) corresponding to the probability of partially observing the sequence $\{\xi_1, \xi_2, \ldots, \xi_t\}$ of length t and of being in state i at time t, see [16].

A target position $\hat{x}$ and target velocity $\hat{\dot{x}}$ to attain are then estimated through *Gaussian Mixture Regression* (GMR) as

$$\hat{x} = \sum_{i=1}^K h_i(\xi) \left(\mu_i^{\mathcal{O}} + \Sigma_i^{\mathcal{O}\mathcal{I}} (\Sigma_i^{\mathcal{I}})^{-1} (\xi^{\mathcal{I}} - \mu_i^{\mathcal{I}}) \right), \tag{5}$$

$$\hat{\dot{x}} = \sum_{i=1}^K h_i(\xi) \left(\mu_i^{\mathcal{O}'} + \Sigma_i^{\mathcal{O}\mathcal{I}'} (\Sigma_i^{\mathcal{I}'})^{-1} (\xi^{\mathcal{I}'} - \mu_i^{\mathcal{I}'}) \right). \tag{6}$$

One advantage of GMR over other regression approaches is that it does not learn a model for a predetermined set of input and output variables. Instead, the joint distribution of the data is first learned by the model through a compact representation encapsulating locally the correlations across the different variables. Regression is then performed by specifying on-the-fly which are the input and output variables, see [13], [14], [17] for details. In the original version of GMR, the weight (4) is computed based on position information only

$$h_i(\xi) = \frac{\mathcal{N}(\xi; \, \mu_i, \Sigma_i)}{\sum_{k=1}^K \mathcal{N}(\xi; \, \mu_k, \Sigma_k)}. \tag{7}$$

We extend here the GMR approach by replacing the weight originally computed through the Gaussian Mixture Model (GMM) representation (7) by its analogous Hidden Markov Model (HMM) representation (4), which encapsulates robustly the sequential nature of the task.

Fig. 2 illustrates the principle of the regression process. From the current position and velocity of the system, a task-level proportional-derivative controller similar to a mass-spring-damper system is computed to reach for the desired velocity $\hat{\dot{x}}$ and for the desired position $\hat{x}$.[4] The acceleration command in task space is determined by

$$\ddot{x} = \overbrace{(\hat{\dot{x}} - \dot{x})\kappa^{\mathcal{V}}}^{\ddot{x}^{\mathcal{V}}} + \overbrace{(\hat{x} - x)\kappa^{\mathcal{P}}}^{\ddot{x}^{\mathcal{P}}}, \tag{8}$$

where $\kappa^{\mathcal{V}}$ and $\kappa^{\mathcal{P}}$ are gains defined as

$$\kappa^{\mathcal{V}} = \frac{1}{\Delta t}, \quad \kappa^{\mathcal{P}}(x) = \kappa_{\max}^{\mathcal{P}} \frac{\mathcal{L}_{\max} - \mathcal{L}(x)}{\mathcal{L}_{\max} - \mathcal{L}_{\min}}, \tag{9}$$

---

[4]Note that this controller also shares similarities with the second-order differential equation defined by a *Vector Integration To Endpoint* (VITE) system [18].

with

$$\mathcal{L}_{\max} = \max_{i \in \{1, K\}} \log \left(\mathcal{N}(\mu_i^x; \mu_i^x, \Sigma_i^x) \right),$$

$$\mathcal{L}_{\min} = \min_{\substack{i \in \{1, K\} \\ x \in \mathcal{W}}} \log \left(\mathcal{N}(x; \mu_i^x, \Sigma_i^x) \right).$$

In the above equation, the notation $\mathcal{L}$ is used to define log-likelihoods (that correspond to weighted distance measures). $\kappa_{\max}^{\mathcal{P}}$ is the maximum gain to attain a target position ($\kappa_{\max}^{\mathcal{P}} = 0.08$ has been fixed empirically). $\mathcal{W}$ defines the robot's workspace, or a predetermined range of situations fixed a priori for the reproduction attempts. Δt is the duration of an iteration step (a constant $\Delta t = 0.01$ is considered here).

At each iteration, $\kappa^{\mathcal{P}}(x)$ is thus close to zero if x is within the boundary determined by the Gaussian distributions (i.e. confidence bounds defined by the centers and covariance matrices). If x is far away from the positions that have been demonstrated, the system comes back towards the closest Gaussian distribution (in a likelihood sense) with a maximum gain of $\kappa_{\max}^{\mathcal{P}}$, still following the trend of motion in this region (determined by $\hat{\dot{x}}$).

Here, velocity and position are updated at each iteration through Euler numerical integration

$$\dot{x}_t = \dot{x}_{t-\Delta t} + \Delta t \, \ddot{x}, \quad x_t = x_{t-\Delta t} + \Delta t \, \dot{x}_t. \tag{10}$$

Note however that other numerical methods for ordinary differential equations can similarly be used here [19]. An inverse kinematics solution that allows to solve a main task and simultaneously takes supplementary constraints into account is then used to control the robot in joint space, as described in [20].

In (8), $\ddot{x}^{\mathcal{V}}$ allows to follow the demonstrated dynamics and $\ddot{x}^{\mathcal{P}}$ prevents the robot from moving far away from an unlearned situation and to come back to an already encountered context if a perturbation occurs. By using both terms concurrently, the robot follows the learned non-linear dynamics while coming back to a known position if it deviates from the demonstrated motion and arrives in a portion of the workspace that remains undiscovered. An illustration of the complete process is presented in Fig. 3. The first row illustrates the process to determine components to reach a desired velocity $\hat{\dot{x}}$ and a desired position $\hat{x}$ through a second order dynamical system. The vector fields in the second row show the influence of the two commands when used separately. On the one hand, $\ddot{x}^{\mathcal{V}}$ follows the learned motion but tends to move away from the demonstrations after a few iterations or by starting from an unexplored position. On the other hand, $\ddot{x}^{\mathcal{P}}$ moves toward the closest point of the generalized trajectory. The vector field in the last row shows the reproduction behavior when considering both commands simultaneously. The final controller follows the demonstrated dynamics and prevents the robot from moving away from an unlearned situation by coming back to an already encountered position if it deviates from the demonstrated motion.

Fig. 4 illustrates the influence of the variability observed during demonstrations for the reproduction attempts. It also
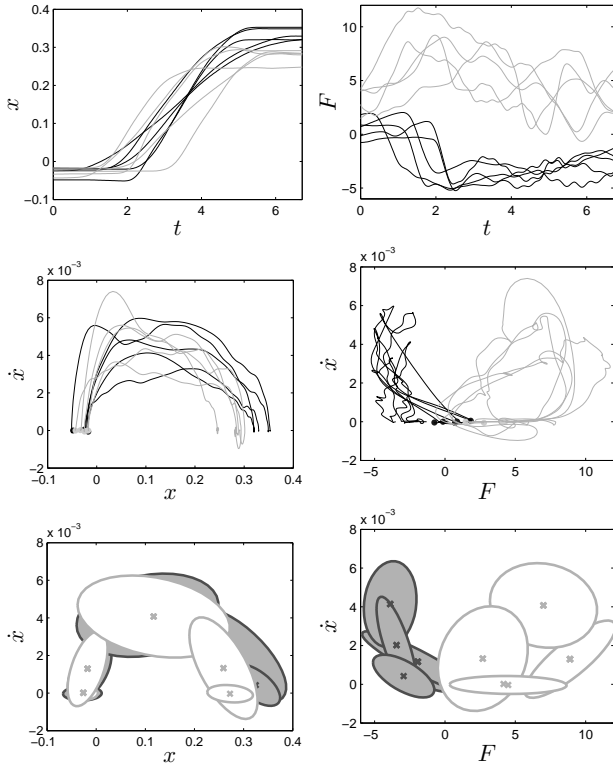
Fig. 5. Demonstrations of the collaborative task to the robot (first two rows) and associated HMM model (last row). The 5 trajectories in black and the 5 trajectories in grey represent respectively the demonstrations of the robot acting as a leader and as a follower. The points represent the beginning of the motions.

shows the evolution of the adaptive gain $\kappa^{\mathcal{P}}$ defined in (9) along the task.

IV. EXPERIMENTAL RESULTS

This experiment aims at validating that the proposed model can distinguish stereotypical following and leading behaviors (i.e. where the user is explicitly told to follow one or the other behavior along the task) and that the model can lead to different controllers during reproduction. This is a first step to determine if the proposed model could address in further work more complex types of behaviors (and switching across those). We assessed the robustness of the proposed system in the series of simulations where different possible input force profiles are fed into the system to modulate the kinematic behavior of the robot.

Fig. 5 shows the demonstrations provided to the robot (first and second row) and the associated HMM models (last row). The dataset and model of the robot acting as a leader (conversely the user acting as a follower) are represented in black line. The dataset and model of the robot acting as a follower (conversely the user acting as a leader) are represented in grey line. In the fourth graph, we see that the correlations between $\dot{x}$ and F change along the motion. In the two situations (leading and following), the correlations can be roughly decomposed into three parts corresponding to the beginning of the motion (user/robot initiating the
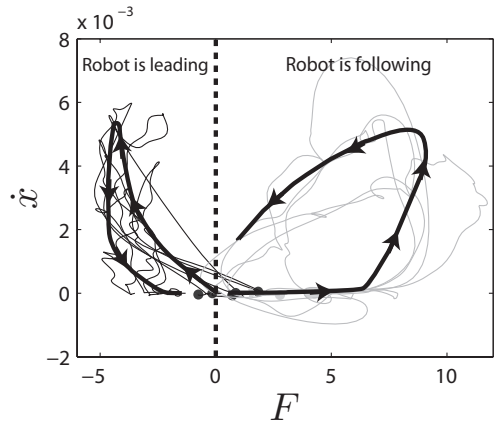

Fig. 6. Illustration of the changes of correlations between force F and velocity $\dot{x}$ along the task. The trajectories in black and grey represent respectively the cases where the robot is leading and following.
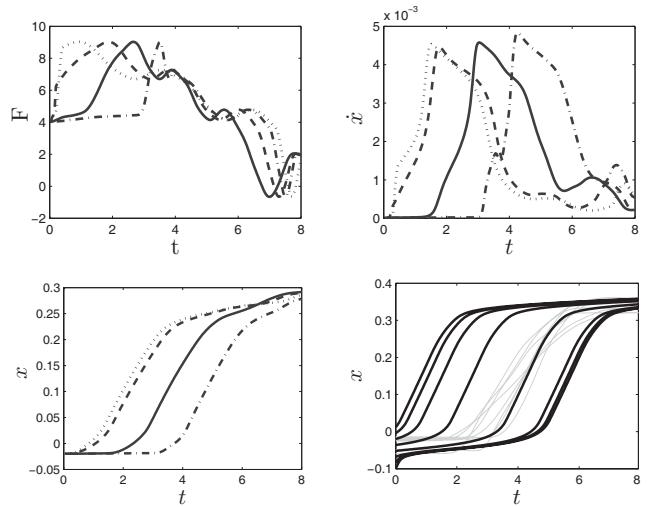

Fig. 7. Reproduction attempts in the case of perturbed force signals (first three graphs) and by starting from different initial positions (last graph).

task), middle of the motion (user and robot lifting the object together) and end of the motion (user/robot notifying the end the task), see also Fig. 6. The first and last datapoints are characterized by a force and velocity close to zero (or moving towards zero). The non-linearities observed along the task show that approximating the collaborative behavior with a system of constant damping factor (i.e. linear relation between force and velocity) would be inefficient to model the collaborative behaviors. We see in the last graph that HMMs can encapsulate compactly and efficiently these different correlations along the motion (two HMMs with 5 states have been used here for the leading and following cases).

Fig. 7 shows reproduction attempts highlighting the robustness of the system to temporal and spatial variability. To highlight the generalization capabilities of the system in terms of temporal variations, the force signal recorded during one of the demonstration (when the robot acts as a follower) is used to simulate the force input during a reproduction attempt. These results are represented in solid

line for the generated force input (first graph), retrieved velocity (second graph) and position (third graph). Three different perturbations of this force signal are then simulated by distorting non-homogeneously in time the original force signal (shown in dashed, dotted, and dash-dotted line). Distorting the signal in such a way simulates situations where the force applied by the user may appear with some temporal variability across the different reproductions. We see that the system successfully adapts to these changes by changing the motion behaviors accordingly. For example, the force input generated in dash-dotted line can represent the behavior of a user first very slow at initiating the task (e.g. the user may not be ready yet), which is reflected by a quasi constant force of $4N$ sensed by the robot (first graph). Then the user suddenly tries to lift the object, that is, after the simulated steady phase, a force signal similar to the demonstration but stretched in time is applied. We see in the second and third graphs that the robot correctly handles this perturbation by staying still first, and then helping the user lift the beam as soon as this one is ready (null velocity for the first one third of the motion). We then see that the the task is collaboratively achieved.

The last graph of Fig. 7 presents reproduction attempts (in black line) where the spatial generalization capabilities of the system are highlighted in the case of the robot acting as a leader. By starting from different initial positions, we see that the system is able to retrieve an appropriate motion to lift the object.

V. CONCLUSIONS AND FURTHER WORK

In this paper we proposed an approach to teach a robot collaborative tasks through a probabilistic model based on Hidden Markov Model and Gaussian Mixture Regression. We emphasized the role that teleoperation holds for transmitting both dynamic and communicative information on the collaborative task, which classical methods of Programming by Demonstration have so far overlooked. We then show through an experiment consisting of lifting an object collaboratively with a humanoid robot that the proposed model can efficiently encapsulate typical communication patterns between different dyads of users acting with stereotypical collaboration behaviors. Reproduction attempts in simulation have finally been presented.

We used here only stereotypical behaviors that were predefined before the interaction between the two users to validate the use of the haptic interface and proposed probabilistic model to record and encode physical collaborative skills. Further work will first concentrate on extending the framework to more natural interactions where the users are not told explicitly to behave with predetermined roles, thus extending the complexity of the haptic communication cues to transfer to the robot. We are currently working on reproducing the learned skill on the real robot, which will be used to evaluate the performance of the proposed controller. We finally plan to contrast the data collected in this experiment with direct recordings of the same dyads of users performing a similar task by endowing the object to lift with force sensors at both extremities, i.e. without passing through the robot and haptic interface to record haptic/kinematics information.

REFERENCES

[1] K. Kosuge, H. Yoshida, and T. Fukuda, "Dynamic control for robot-human collaboration," in *Proceedings of the 2nd IEEE International Workshop on Robot and Human Communication*, Tokyo, Japan, 1993, pp. 389–401.

[2] H. Arai, T. Takubo, Y. Hayashibara, and K. Tanie, "Human-robot cooperative manipulation using a virtual nonholonomic constraint," in *Proc. IEEE Intl Conf. on Robotics and Automation (ICRA)*, April 2000, pp. 4064–4070.

[3] Y. Hirata, Y. Kume, Z.-D. Wang, and K. Kosuge, "Decentralized control of multiple mobile manipulators based on virtual 3D caster motion of handling an object in cooperation with a human," in *Proc. IEEE Intl Conf. on Robotics and Automation (ICRA)*, September 2003, pp. 938–943.

[4] S. Yigit, C. Burghart, and H. Worn, "Cooperative carrying using pump-like constraints," in *Proc. IEEE/RSJ Intl Conf. on Intelligent Robots and Systems (IROS)*, September–October 2004, pp. 3877–3882.

[5] T. Tsumugiwa, R. Yokogawa, and K. Hara, "Variable impedance control with regard to working process for man-machine cooperation-work system," in *Proc. IEEE/RSJ Intl Conf. on Intelligent Robots and Systems (IROS)*, October–November 2001, pp. 1564–1569.

[6] V. Duchaine and C. Gosselin, "General model of human-robot cooperation using a novel velocity based variable impedance control," in *Joint EuroHaptics Conference and Symposium on Haptic Interfaces for Virtual Environment and Teleoperator Systems*, 2007, pp. 446–451.

[7] A. Billard, S. Calinon, R. Dillmann, and S. Schaal, "Robot programming by demonstration," in *Handbook of Robotics*, B. Siciliano and O. Khatib, Eds. Secaucus, NJ, USA: Springer, 2008, pp. 1371–1394.

[8] Z.-D. Wang, Y. Takano, Y. Hirata, and K. Kosuge, "A pushing leader based decentralized control method for cooperative object transportation," in *Proc. IEEE/RSJ Intl Conf. on Intelligent Robots and Systems (IROS)*, September–October 2004, pp. 1035–1040.

[9] M. Rahman, R. Ikeura, and K. Mizutani, "Control characteristics of two humans in cooperative task," in *IEEE Intl Conf. on Systems, Man, and Cybernetics*, vol. 2, 2000, pp. 1301–1306.

[10] S. Gentry and E. Feron, "Musicality experiments in lead and follow dance," in *IEEE Intl Conf. on Systems, Man, and Cybernetics*, vol. 1, 2004, pp. 984–988.

[11] K. Reed and M. Peshkin, "Physical collaboration of human-human and human-robot teams," *IEEE Transactions on Haptics*, vol. 1, no. 2, pp. 108–120, December 2008.

[12] P. Evrard and A. Kheddar, "Homotopy switching model for dyad haptic interaction in physical collaborative tasks," in *Joint Eurohaptics Conference and Symposium on Haptic Interfaces for Virtual Environment and Teleoperator Systems (WorldHaptics 2009)*, Salt Lake City, USA, March 2009.

[13] M. Hersch, F. Guenter, S. Calinon, and A. Billard, "Dynamical system modulation for robot learning via kinesthetic demonstrations," *IEEE Trans. on Robotics*, vol. 24, no. 6, pp. 1463–1467, 2008.

[14] S. Calinon, F. Guenter, and A. Billard, "On learning, representing and generalizing a task in a humanoid robot," *IEEE Trans. on Systems, Man and Cybernetics, Part B*, vol. 37, no. 2, pp. 286–298, 2007.

[15] Z. Wang, A. Peer, and M. Buss, "An HMM approach to realistic haptic human-robot interaction," in *Joint EuroHaptics Conference and Symposium on Haptic Interfaces for Virtual Environment and Teleoperator Systems*, 2009, pp. 374–379.

[16] L. Rabiner, "A tutorial on hidden Markov models and selected applications in speech recognition," *Proc. IEEE*, vol. 77:2, pp. 257–285, February 1989.

[17] Z. Ghahramani and M. Jordan, "Supervised learning from incomplete data via an EM approach," in *Advances in Neural Information Processing Systems*, J. D. Cowan, G. Tesauro, and J. Alspector, Eds., vol. 6. Morgan Kaufmann Publishers, Inc., 1994, pp. 120–127.

[18] D. Bullock and S. Grossberg, "Neural dynamics of planned arm movements: Emergent invariants and speed-accuracy properties during trajectory formation," *Psychological Review*, vol. 95, no. 1, pp. 49–90, 1988.

[19] J. Butcher, *Numerical Methods for Ordinary Differential Equations*. Chichester, UK: Wiley, 2003.

[20] N. Mansard, O. Khatib, and A. Kheddar, "Integrating unilateral constraints inside the stack of tasks," *IEEE Trans. on Robotics*, 2009, in press.